

Gluon radiation & QCD at the LHC

Jeff Forshaw

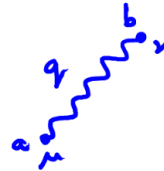
Overview

1. Introduction to perturbative QCD
2. Fixed order calculations at the LHC
3. All order calculations and resummation
4. The menace of Coulomb gluons
5. Using QCD to probe new physics

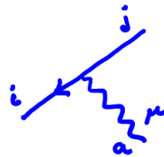
$$\mathcal{L} = \bar{\Psi} i \gamma_\mu D^\mu \Psi - \frac{1}{4} F_{\mu\nu}^a F^{\mu\nu}_a$$



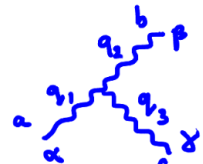
$$\frac{i \delta_{ij}}{\not{p} - m + i\epsilon}$$



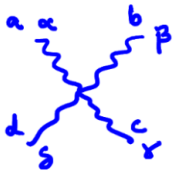
$$\frac{i}{q^2 + i\epsilon} d_{\mu\nu} \delta_{ab}$$




$$-ig T_{ij}^a \gamma_\mu$$




$$-ig (ifabc) \{ g_{\alpha\beta} (q_1 - q_2)_\gamma + g_{\beta\gamma} (q_2 - q_3)_\alpha + g_{\gamma\alpha} (q_3 - q_1)_\beta \}$$



$$-ig^2 \{ f_{abc} f_{cde} (g_{\mu\nu} g_{\rho\sigma} - g_{\mu\sigma} g_{\rho\nu}) + f_{ace} f_{bde} (g_{\mu\rho} g_{\nu\sigma} - g_{\mu\sigma} g_{\rho\nu}) + f_{ade} f_{abc} (g_{\mu\sigma} g_{\nu\rho} - g_{\mu\rho} g_{\nu\sigma}) \}$$



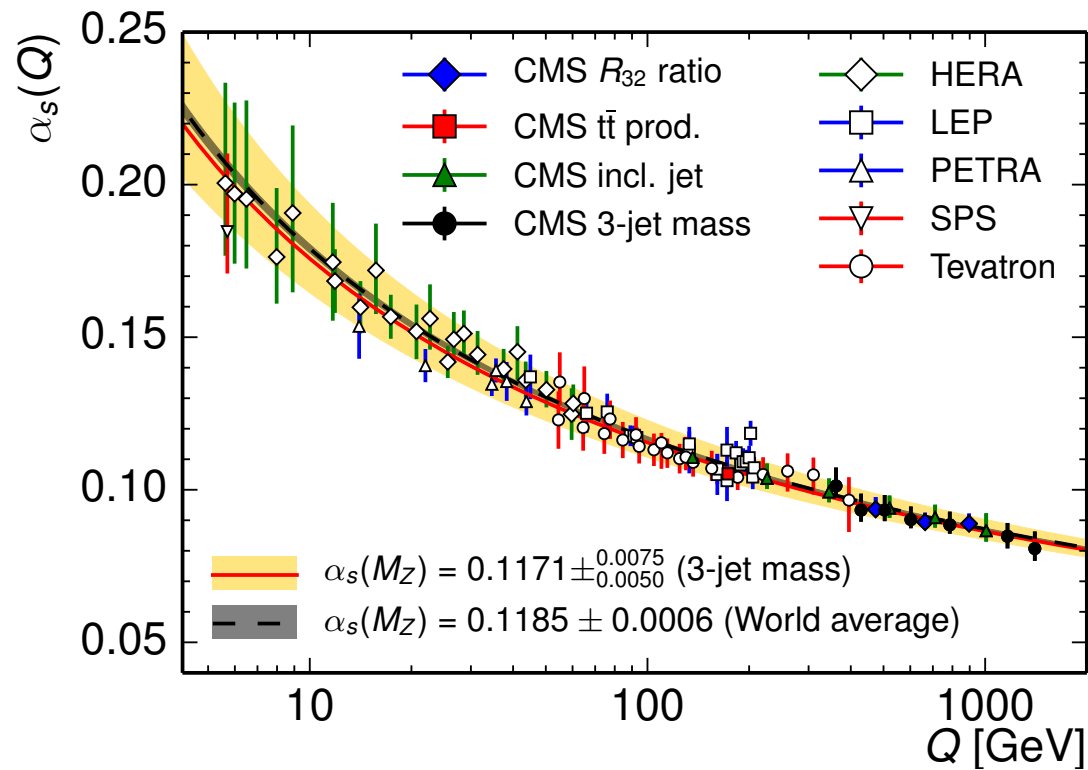
$$\frac{i}{q^2 + i\epsilon} \delta_{ab}$$



$$-ig q_\mu (-ifabc)$$

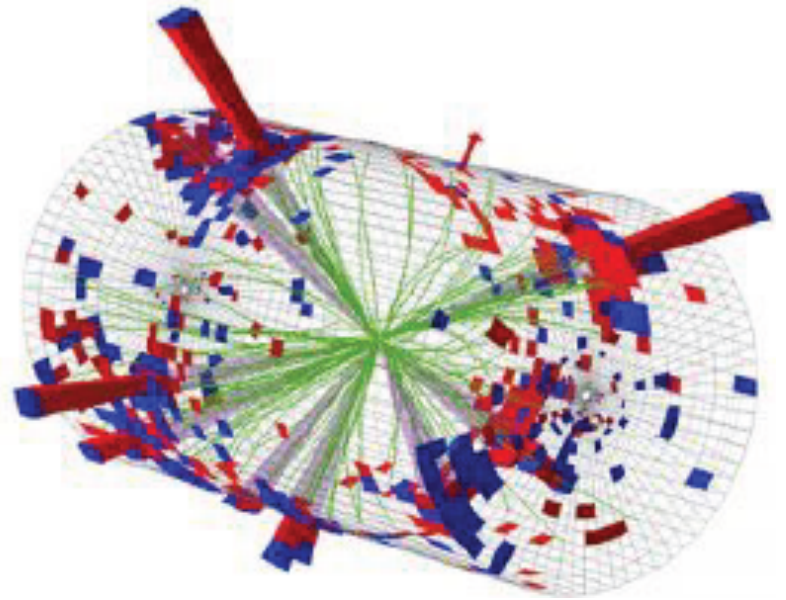
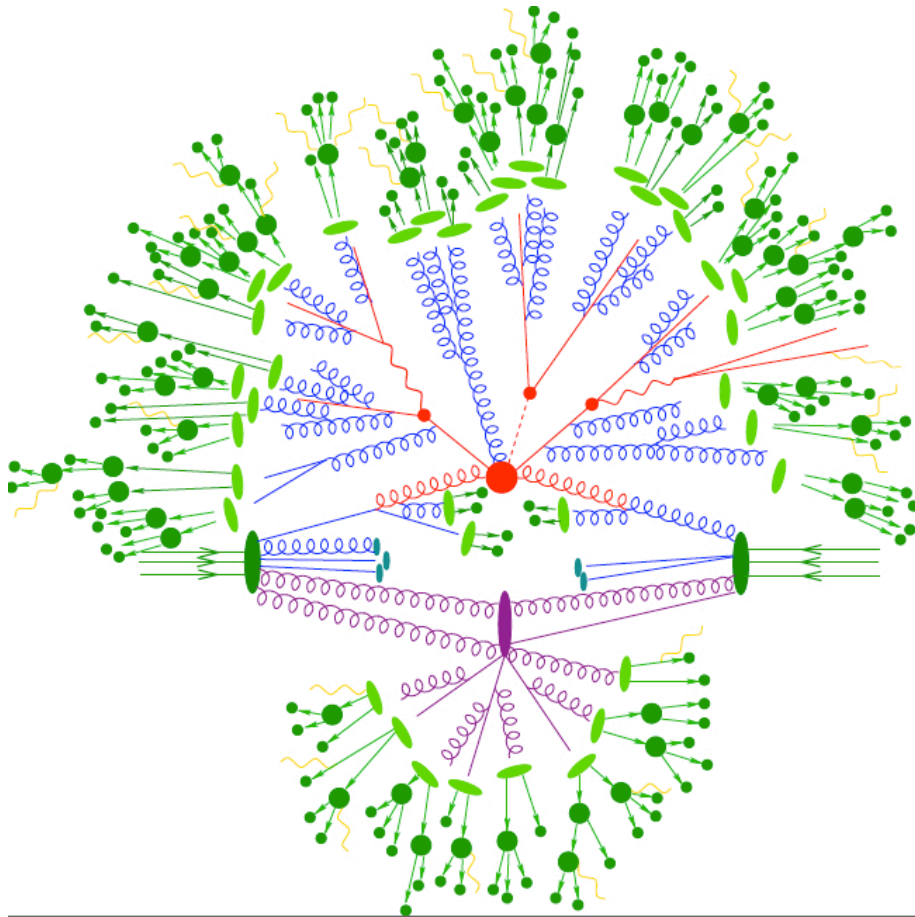
Asymptotic Freedom

$$\alpha_s = \frac{g^2}{4\pi}$$



Free quarks and gluons do not exist.

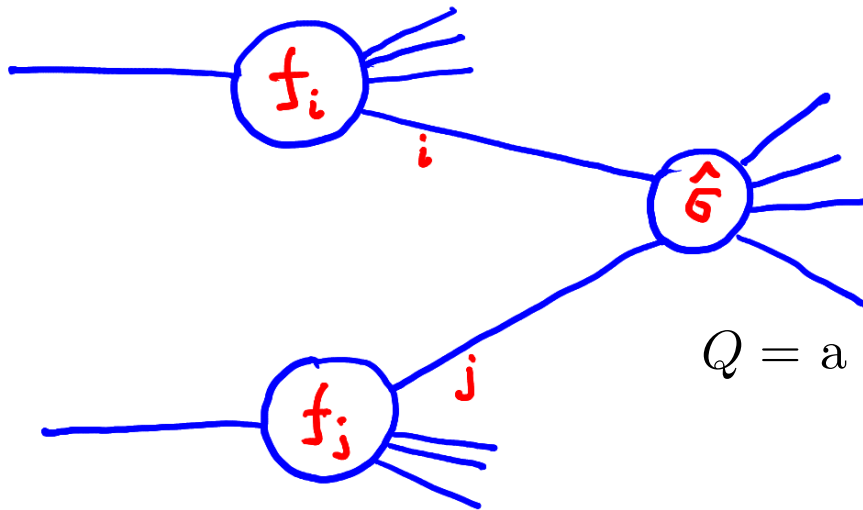
But we can use pQCD to describe their interactions at short distances.



Factorization allows us to make predictions

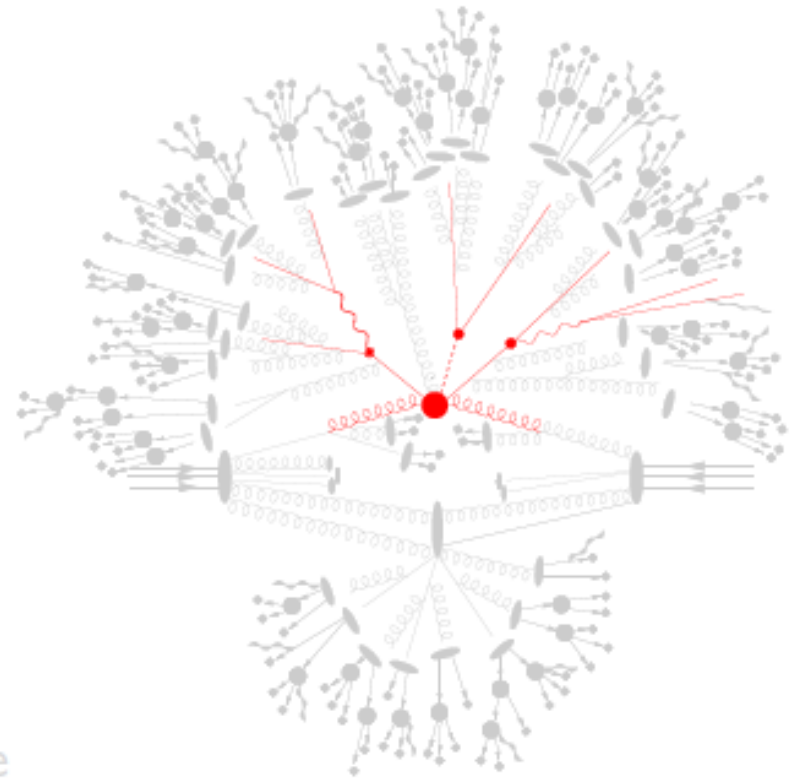
$$d\sigma = \sum_{i,j} \int dx_1 dx_2 f_i(x_1, \mu_F) f_j(x_2, \mu_F) d\hat{\sigma}_{ij}(Q, \mu_R, \mu_F)$$

f_i is a universal function



$Q =$ a large invariant mass.

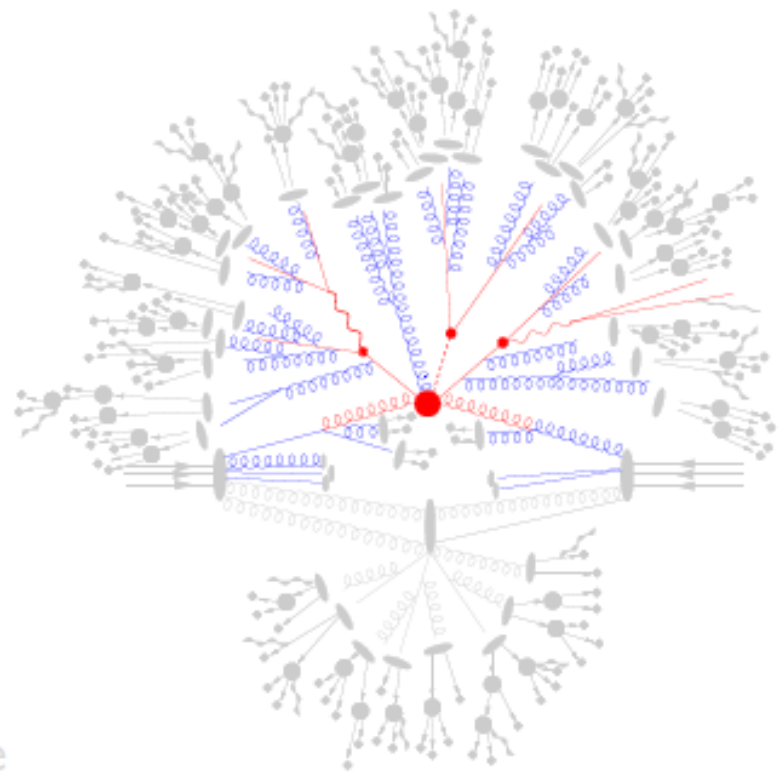
- ▶ Short distance interactions
 - ▶ Signal process
 - ▶ Radiative corrections
- ▶ Long-distance interactions
 - ▶ Hadronization
 - ▶ Particle decays



Factorization

- ▶ Quantity of interest: Total interaction rate
- ▶ Convolution of short & long distance physics

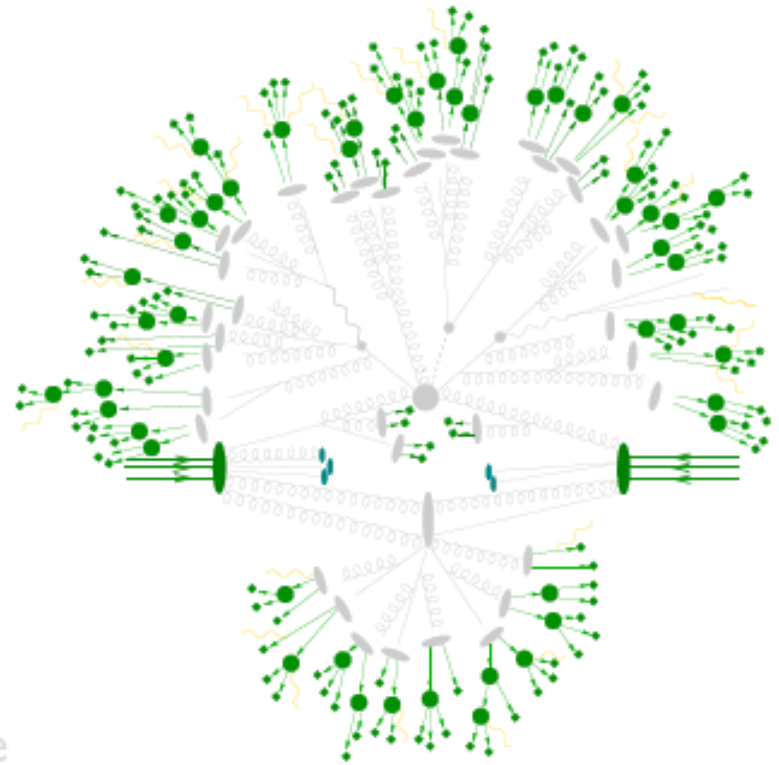
- ▶ Short distance interactions
 - ▶ Signal process
 - ▶ Radiative corrections
- ▶ Long-distance interactions
 - ▶ Hadronization
 - ▶ Particle decays



Factorization

- ▶ Quantity of interest: Total interaction rate
- ▶ Convolution of short & long distance physics

- ▶ Short distance interactions
 - ▶ Signal process
 - ▶ Radiative corrections
- ▶ Long-distance interactions
 - ▶ Hadronization
 - ▶ Particle decays

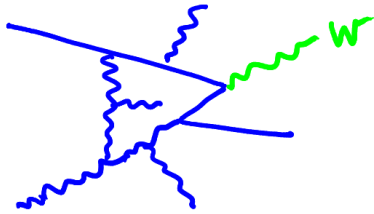


Factorization

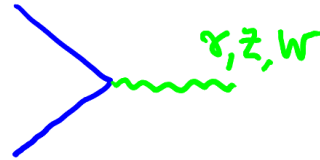
- ▶ Quantity of interest: Total interaction rate
- ▶ Convolution of short & long distance physics

$$\hat{\sigma} \sim \alpha_s^n \left(\hat{\sigma}_{LO} + \alpha_s \hat{\sigma}_{NLO} + \alpha_s^2 \hat{\sigma}_{NNLO} + \alpha_s^3 \hat{\sigma}_{NNNLO} + \dots \right)$$

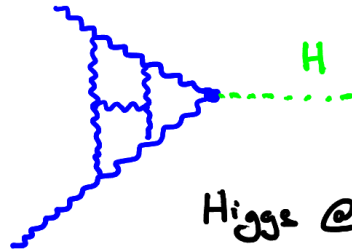
↑
order of magnitude
↑
automation
↑
state of art
↑
world record in QCD



W + 4 jets @ NLO
[2010]
n = 4

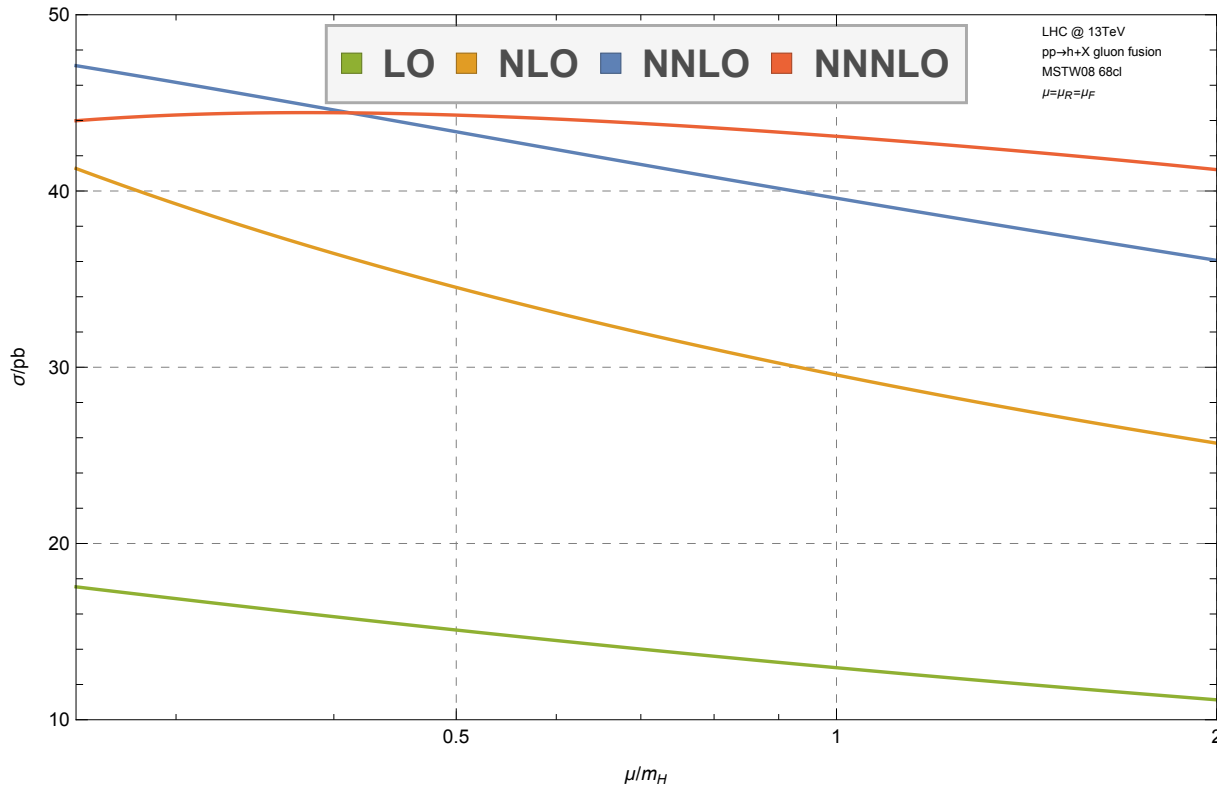


Drell-Yan @ LO
n = 0



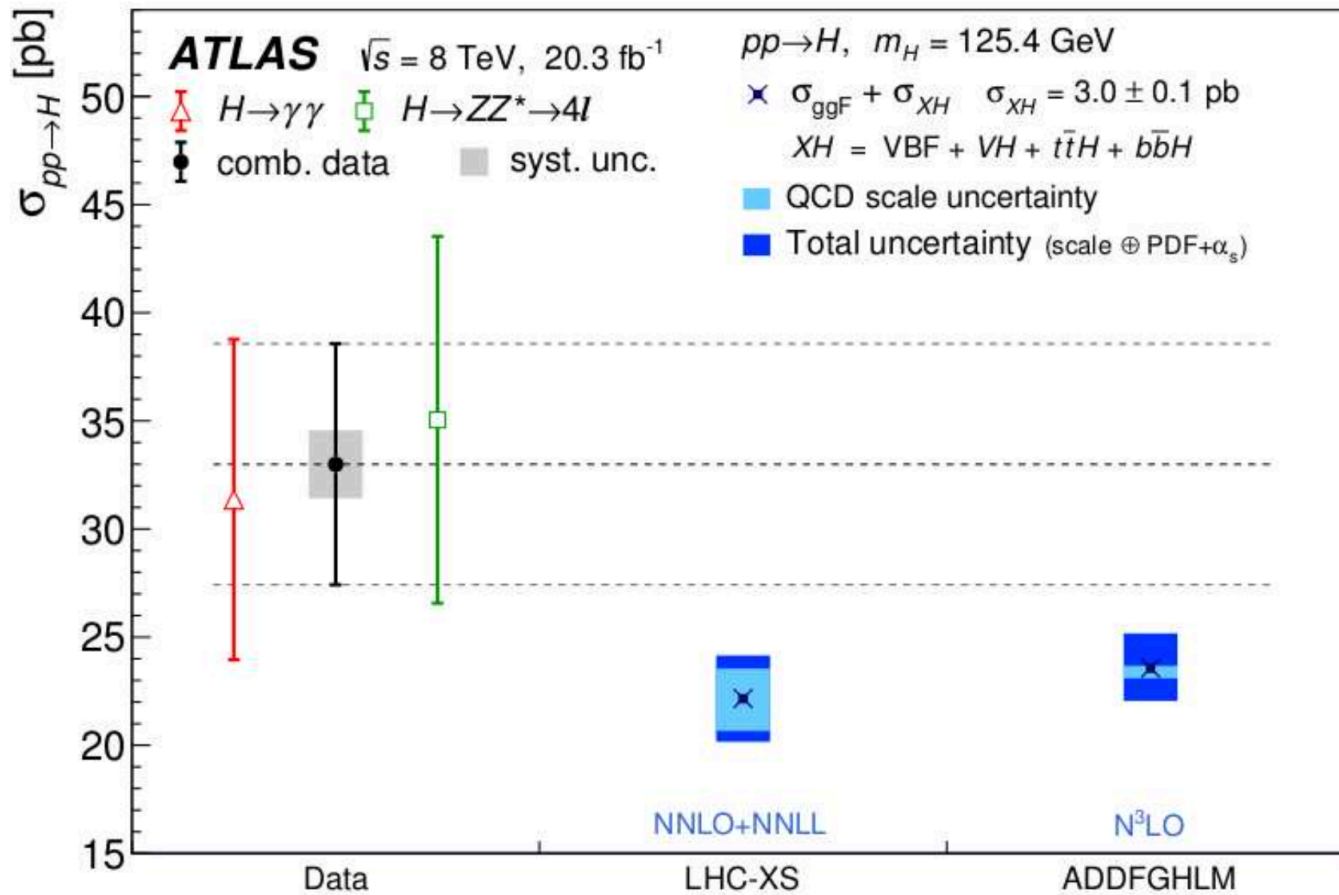
Higgs @ N3LO
~ 10⁵ Feynman diagrams
~ 1/2 billion integrals

QCD Higgs production at three loops

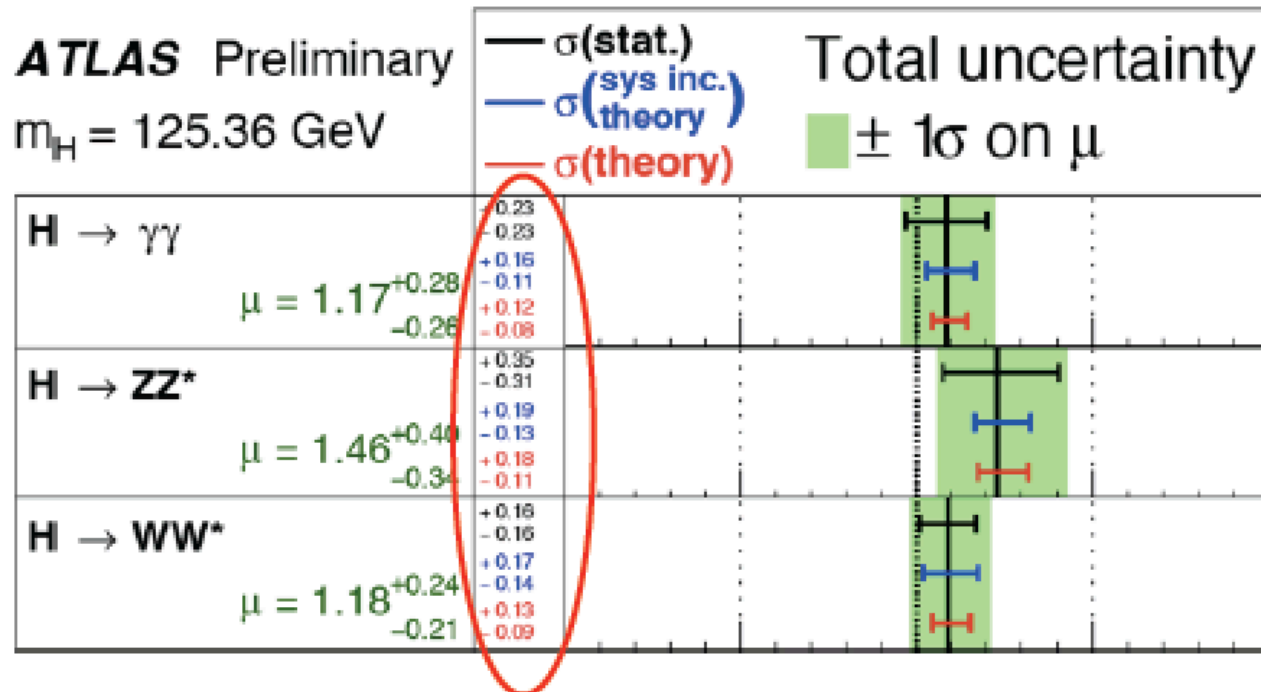


“The total scale variation at N3LO is 3%, reducing the uncertainty due to missing higher order QCD corrections by a factor of three.”

σ/pb	2 TeV	7 TeV	8 TeV	13 TeV	14 TeV
$\mu = \frac{m_H}{2}$	$0.99^{+0.43\%}_{-4.65\%}$	$15.31^{+0.31\%}_{-3.08\%}$	$19.47^{+0.32\%}_{-2.99\%}$	$44.31^{+0.31\%}_{-2.64\%}$	$49.87^{+0.32\%}_{-2.61\%}$
$\mu = m_H$	$0.94^{+4.87\%}_{-7.35\%}$	$14.84^{+3.18\%}_{-5.27\%}$	$18.90^{+3.08\%}_{-5.02\%}$	$43.14^{+2.71\%}_{-4.45\%}$	$48.57^{+2.68\%}_{-4.24\%}$

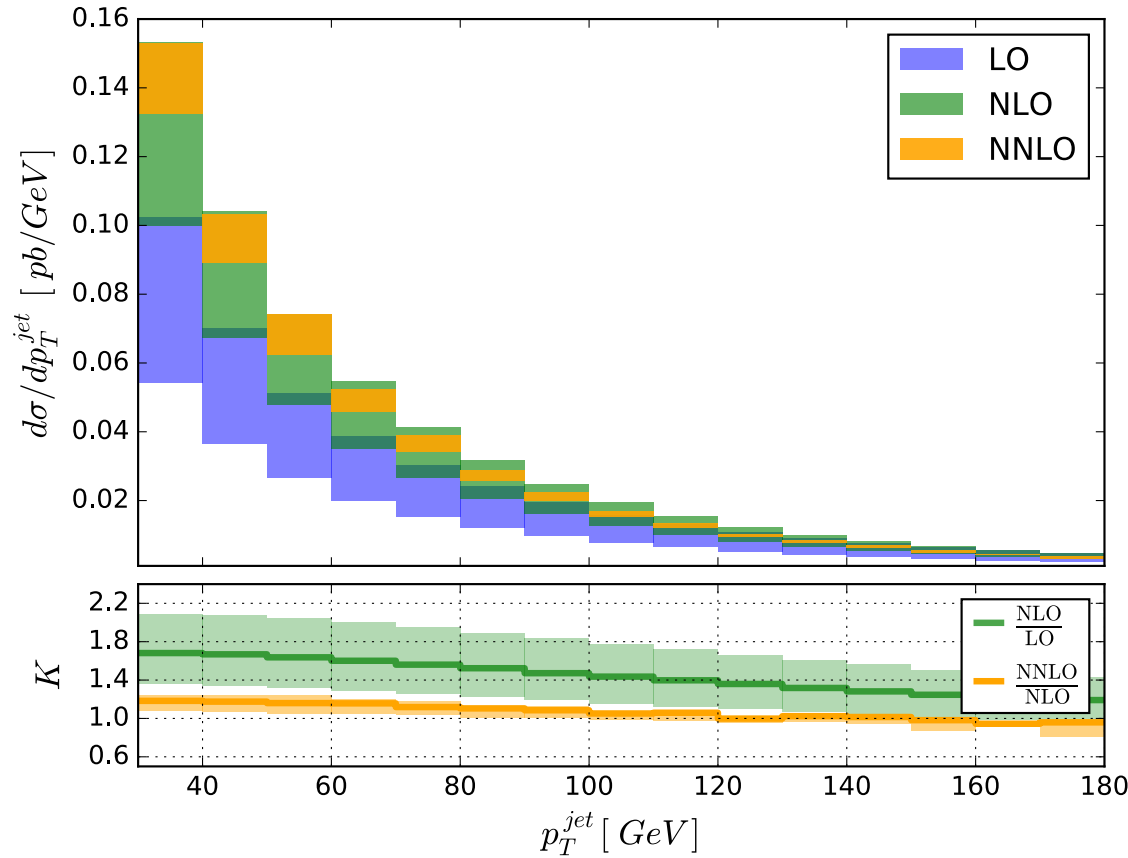


- There will be a continued need for further improvements in precision QCD as Run II data arrives.



- The dominant component of the systematic error on the signal strength is theory.
- This will become a limiting factor in interpretation in Run II as statistical errors decrease.

Need better theory to sharpen our probes of BSM physics
in the Higgs sector!



Higgs + 1 jet

NNLO

$p_T^{jet} > 30 \text{ GeV}, Y^{jet} < 2.5$	
Leading order:	$3.1^{+1.3}_{-0.9} \text{ pb}$
Next-to-leading order:	$4.8^{+1.1}_{-0.9} \text{ pb}$
Next-to-next-to-leading order:	$5.5^{+0.3}_{-0.4} \text{ pb}$

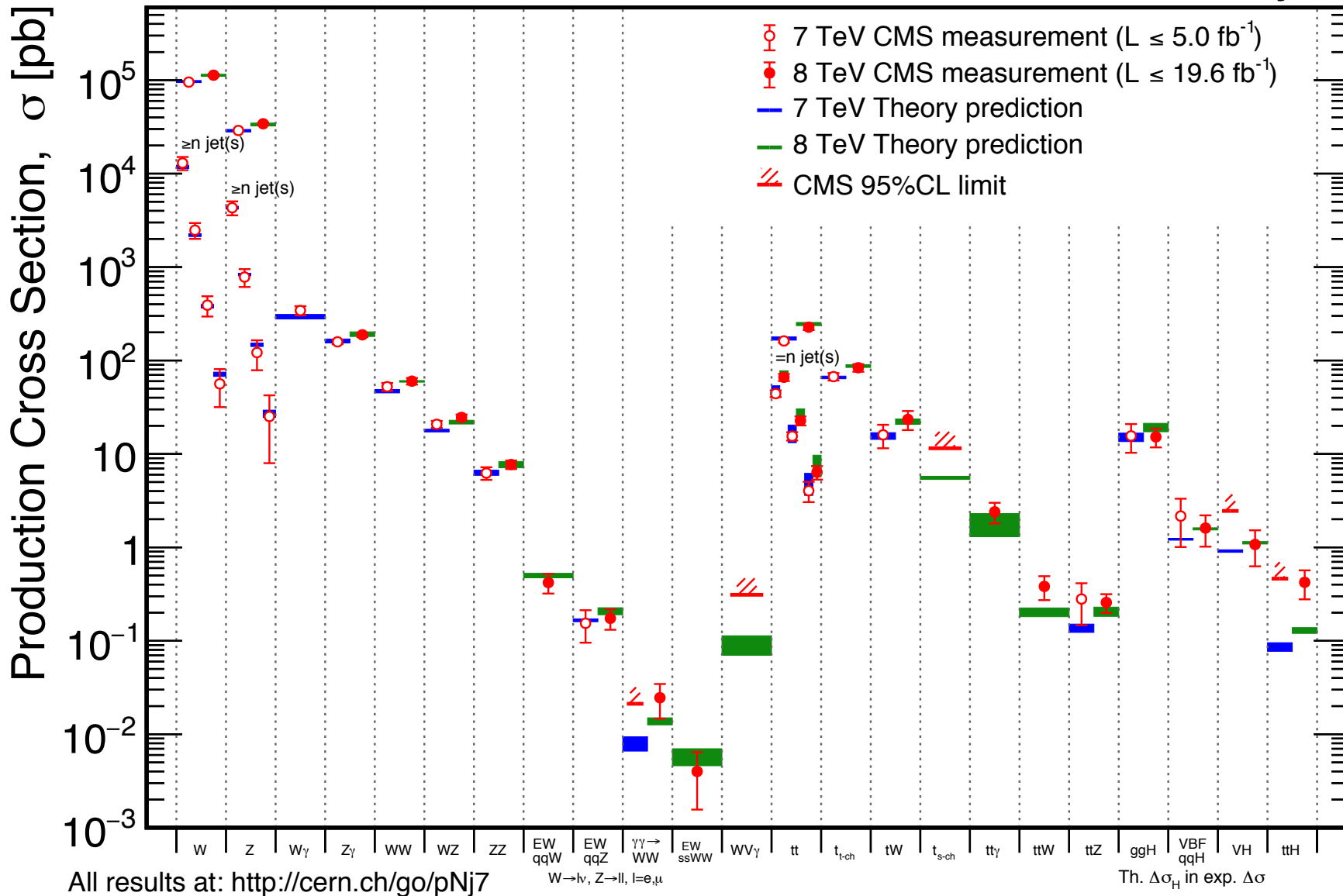
Table I: Fiducial cross sections, defined by $p_T^{jet} > 30 \text{ GeV}$, $|Y^{jet}| < 2.5$, using NNPDF PDFs at each order of perturbation theory. The central scale choice is $\mu = m_H$. Results for $\mu = m_H/2$ and $\mu = 2m_H$ are shown as superscripts and subscripts, respectively.

Boughezal, Focke, Giele, Liu, Petriello
[arXiv:1505.03893](https://arxiv.org/abs/1505.03893)

Precision at the LHC

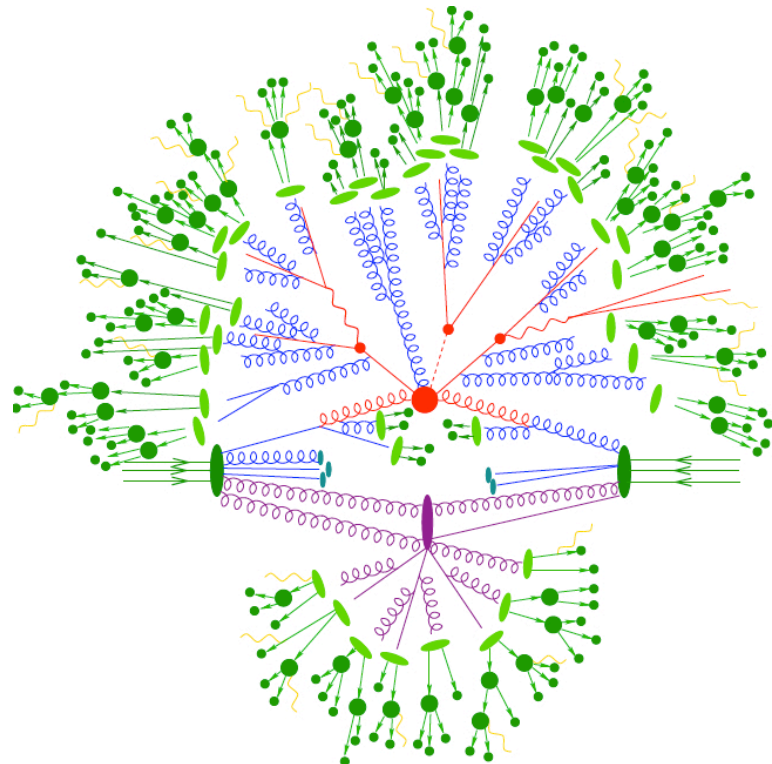
July 2015

CMS Preliminary

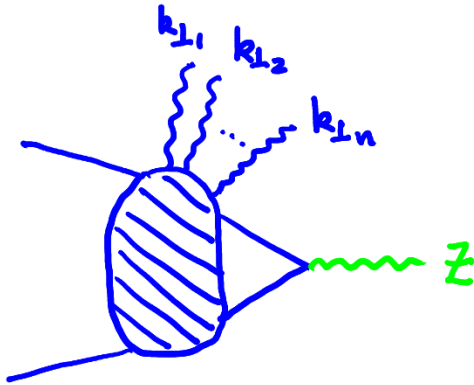


Many observables are (often by construction) sensitive to multiparticle production in the final state.

The production of many particles is typically not rare: the rate is enhanced by large logarithmic terms in the perturbation series.



A classic example: Drell-Yan



$$\frac{d\sigma}{dp_T} = \frac{d}{dp_T} \left(\sigma_0 \exp \left(-\frac{\alpha_s C_F}{2\pi} L^2 \right) \right)$$

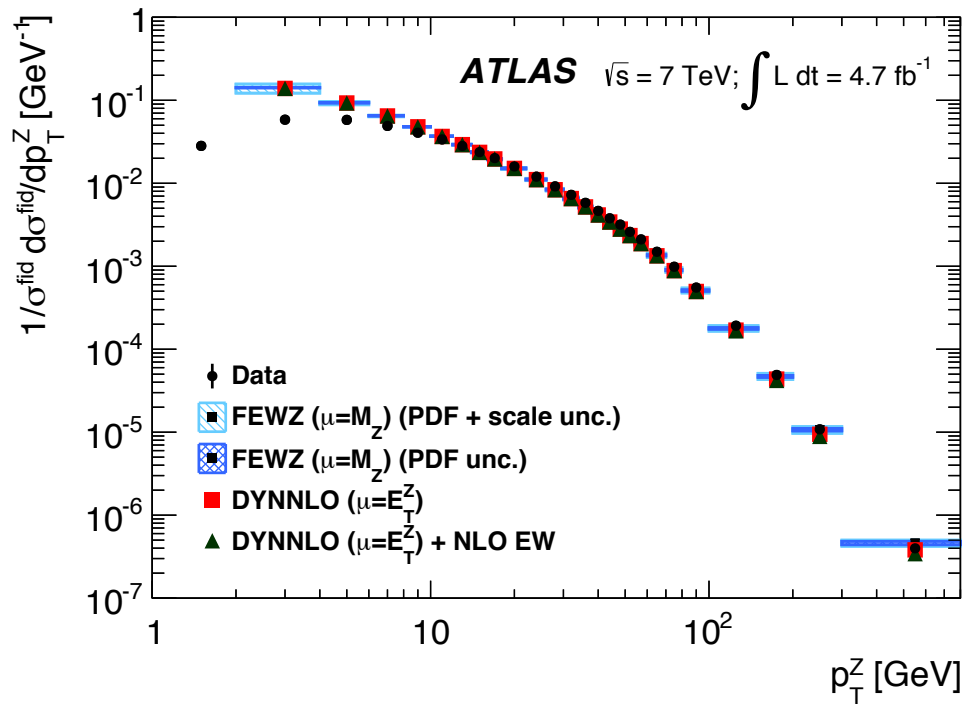
p_T = transverse momentum of the Z particle

$$L = \ln(Q^2/p_T^2)$$

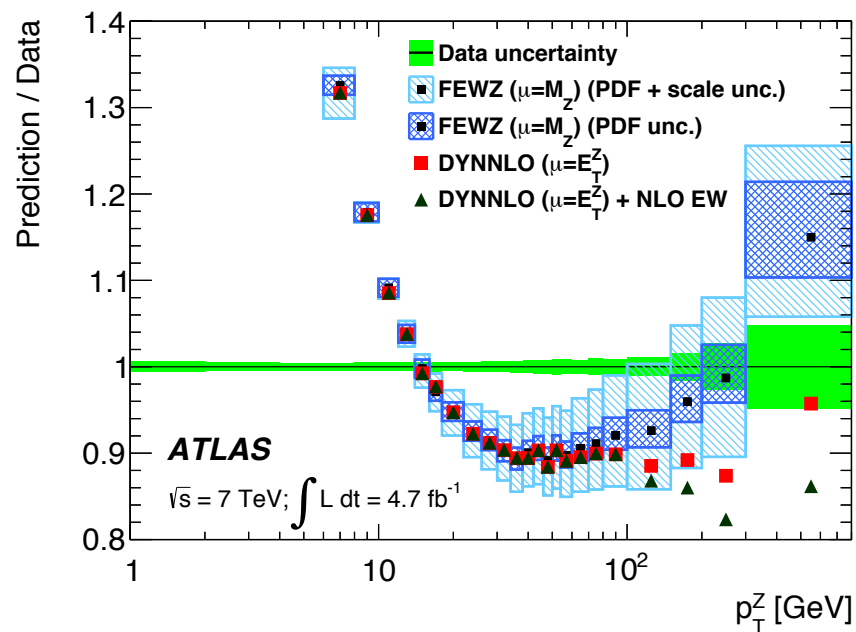
- Fixed order in α_s fails if $L \gg 1$.
- Accounts for all terms $\sim \alpha_s^n L^{2n}$.
- Simple interpretation as a non-emission probability.

$$\int_0^{p_T} \frac{d\sigma}{dp'_T} dp'_T = \sigma_0 \exp \left(-\frac{\alpha_s C_F}{2\pi} L^2 \right)$$

= rate of producing Z particles with transverse momentum below p_T



NNLO fails at low p_T



Beyond the simplest approximation: systematic resummation of the large logarithms is possible.

$$\mathcal{O} = 1 + \alpha_s(L^2 + L + 1) + \alpha_s^2(L^4 + L^3 + L^2 + L + 1) + \dots$$

For many observables:

$$\mathcal{O} = C(\alpha_s) \exp \left[Lg_{LL}(\alpha_s L) + g_{NLL}(\alpha_s L) + \alpha_s g_{NNLL}(\alpha_s L) + \dots \right]$$

$$C(\alpha_s) = 1 + \alpha_s C_{NNLL} + \dots$$

Can match the resummed result with the fixed order result.

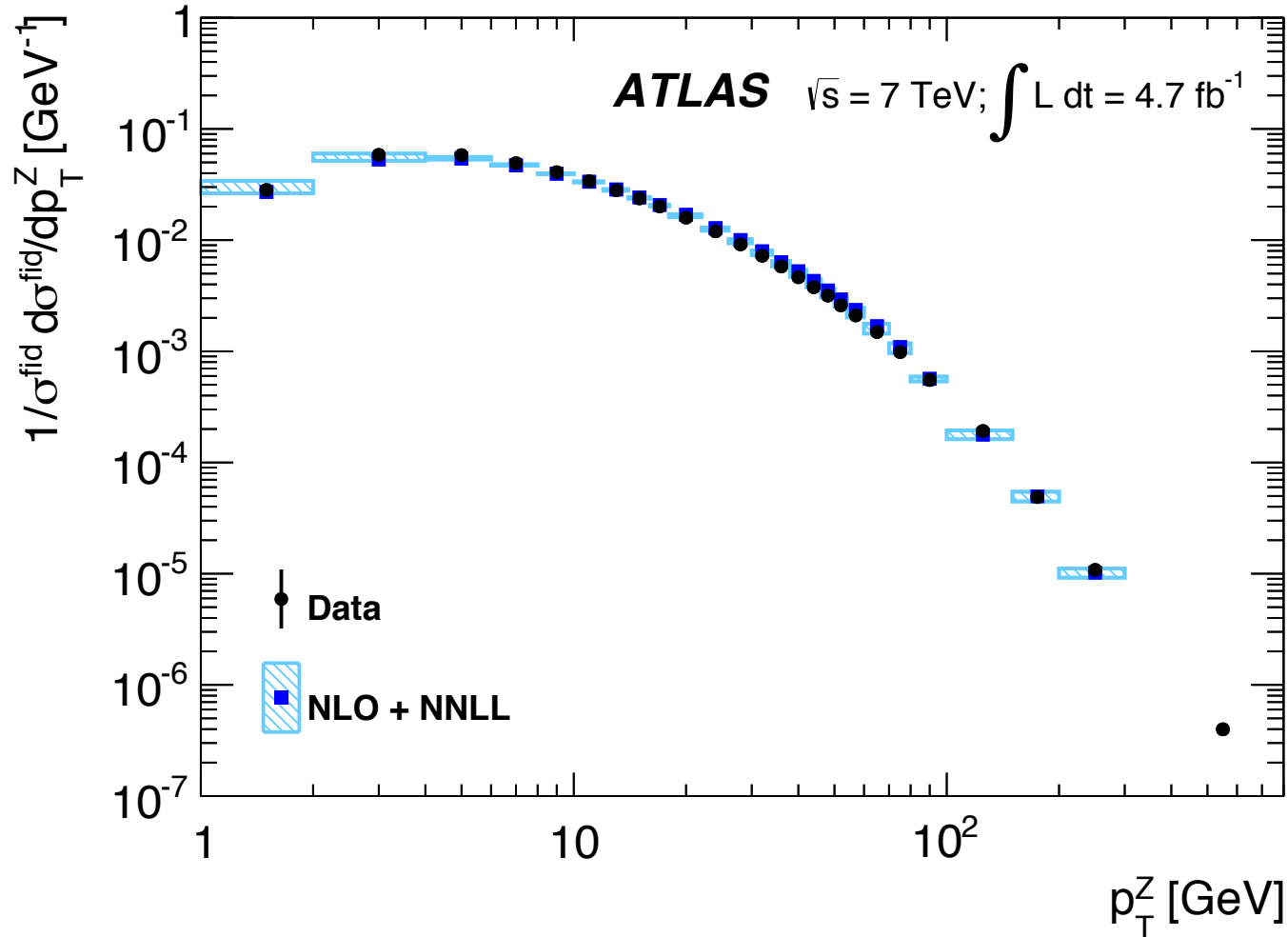
Progress in automated resummation

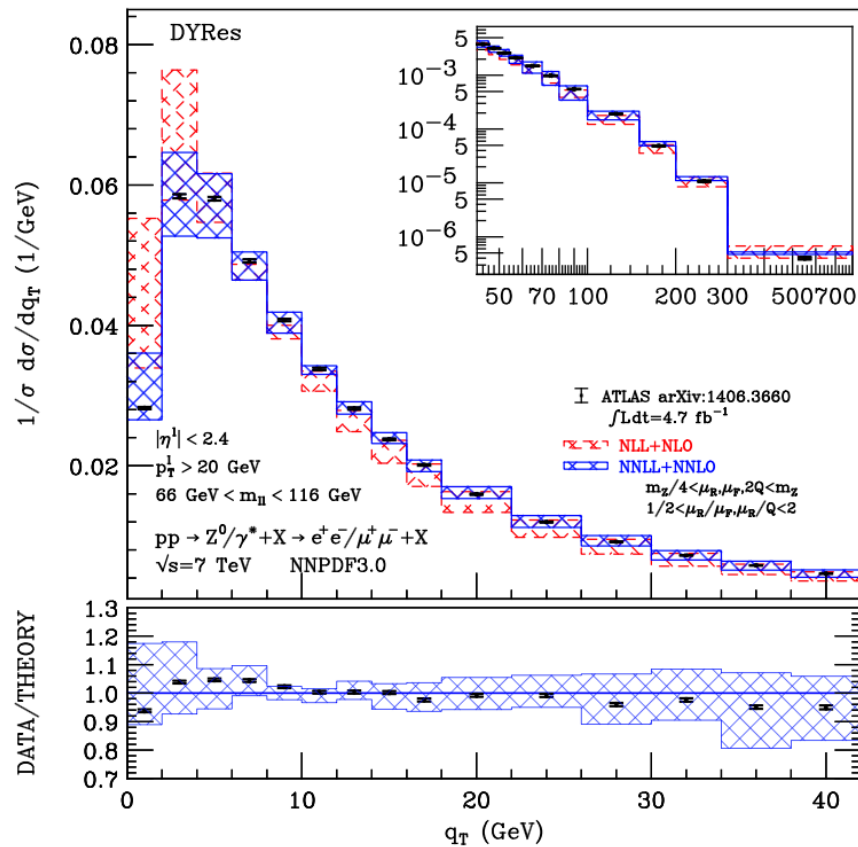
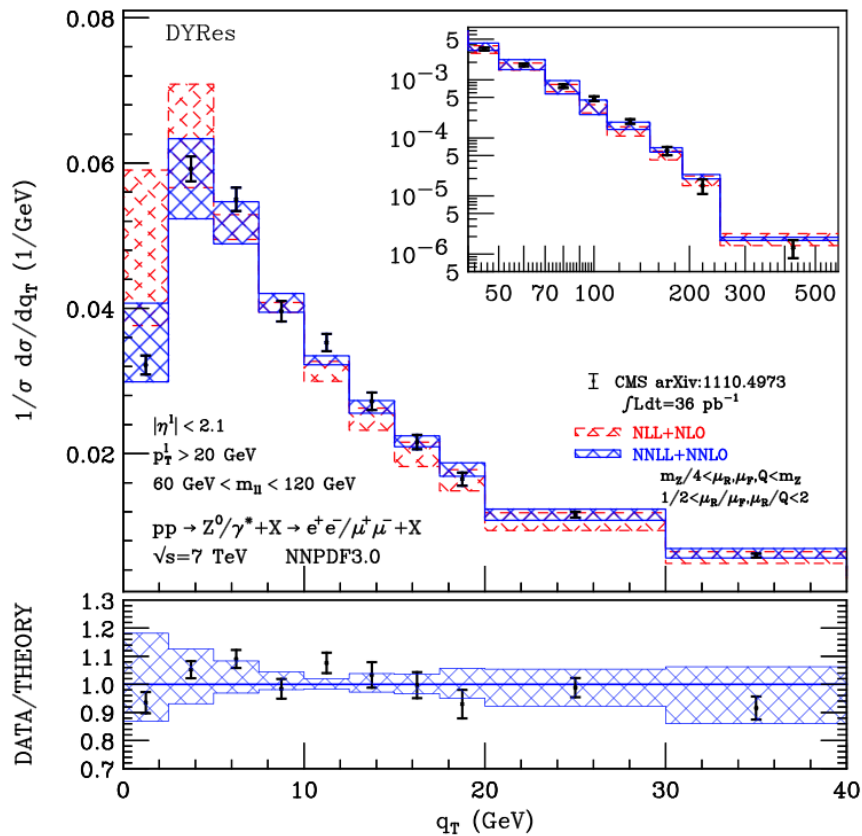
e^+e^- at NLL: Banfi, Salam, Zanderighi hep-ph//0407286

e^+e^- at NNLL: Banfi, McAslan, Monni, Zanderighi arXiv:1412.2126

Gerwick, Schumann, Höche, Marzani arXiv: 1411.7325

All orders (resummed) works well

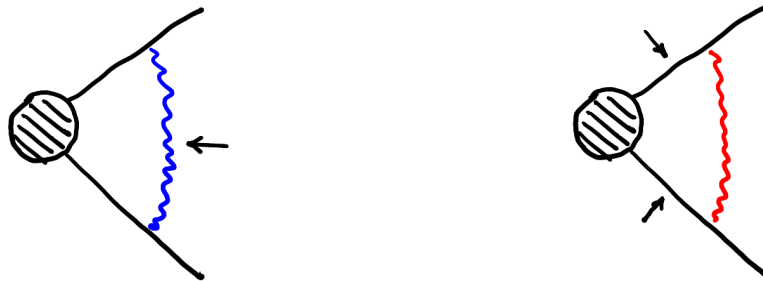




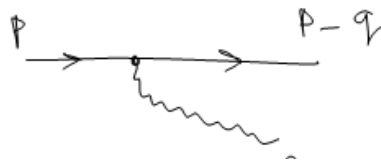
NNLO + NNLL

The large logarithms of infra-red origin are a result of:

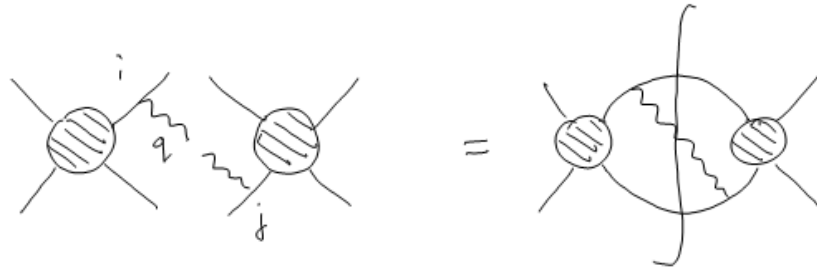
1. Soft gluon emission
2. Collinear parton branching



SOFT GLUONS



$$= 2gp_\mu \delta_{\lambda\lambda'} T_{ij}^a$$

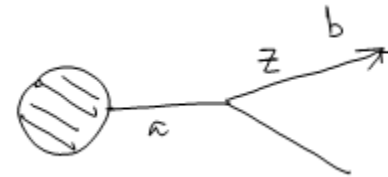


$$d\sigma_{n+1} = d\sigma_n \frac{\alpha_s}{2\pi} \frac{dE}{E} \frac{d\Omega}{2\pi} \sum_{ij} C_{ij} E^2 \frac{p_i \cdot p_j}{p_i \cdot q p_j \cdot q}$$

- Only have to consider soft gluons off the external legs of a hard subprocess.
- Colour factor is the “problem”.

COLLINEAR EMISSIONS

Colour structure is easier. It is as if emission is off the parton to which it is collinear.



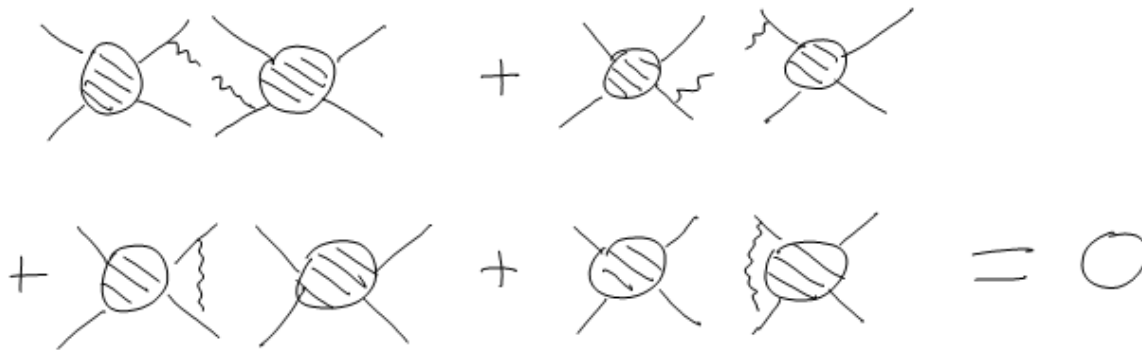
$$d\sigma_{n+1} = d\sigma_n \frac{\alpha_s}{2\pi} \frac{dq^2}{q^2} dz P_{ba}(z)$$

Simulation codes exploit the fact that in the “large N_c ” approximation both wide-angle soft and collinear emissions can be included via a classical branching algorithm.

Not all observables are affected by soft and/or collinear enhancements

Intuitive: inclusive observables do not care that the outgoing partons may subsequently radiate additional soft and/or collinear particles.

Bloch-Nordsieck Theorem



Real & virtual graphs cancel exactly in soft approximation if the real emissions are integrated over without restriction.

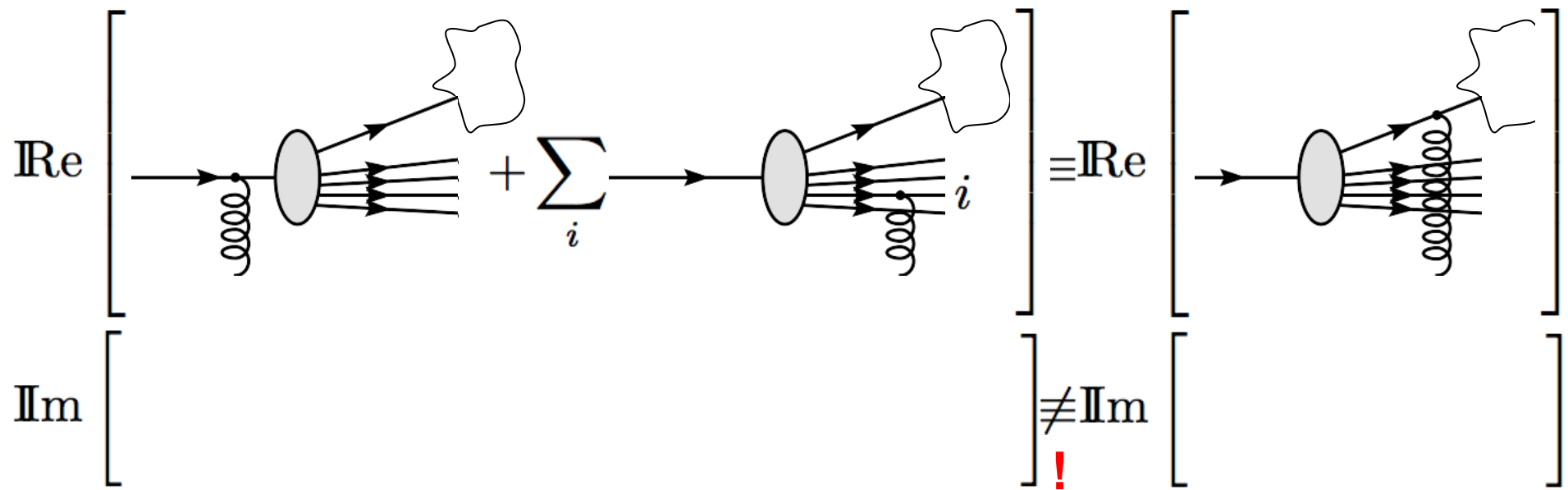
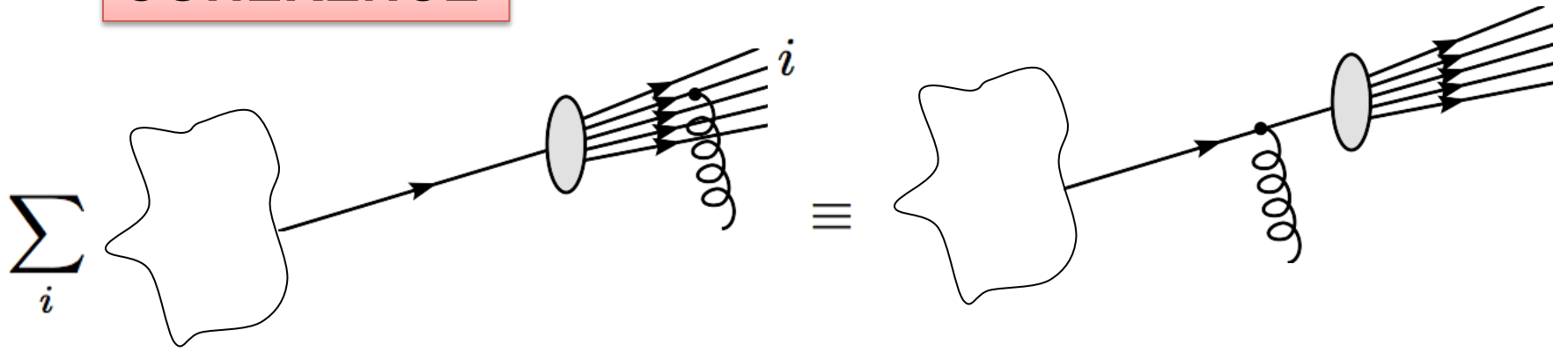
Weighting the real emissions induces a miscancellation and a logarithm, e.g.

$$\alpha_s \int_0^Q \frac{dk_T}{k_T} - \alpha_s \int_0^\mu \frac{dk_T}{k_T} = \alpha_s \ln \frac{Q}{\mu}$$

Virtual loop

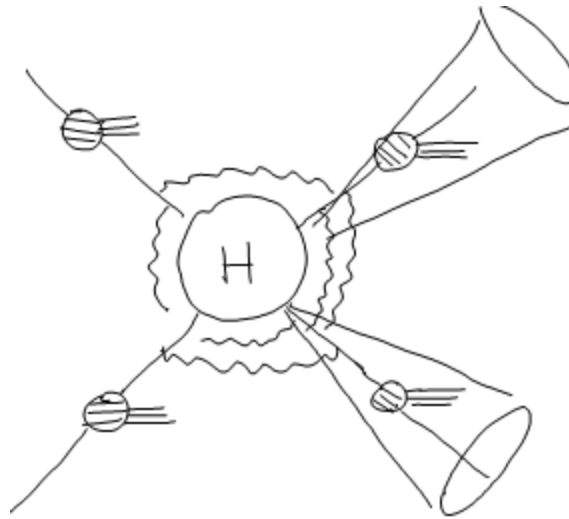
Real emission phase-space if emissions forbidden above μ

COHERENCE



COHERENCE

Used to factorize collinear emissions from soft, wide angle, gluon emissions.



The failure of the “coherence identity” for the imaginary part will be significant later.

Soft gluon corrections will be important for observables that measure only *small deviations from lowest order kinematics*.

In such cases real radiation is constrained to a small corner of phase space and BN miscancellation triggers large logarithms.

If V measures 'distance' from the lowest order kinematics:

Event shapes such as thrust ($V = 1 - T$)

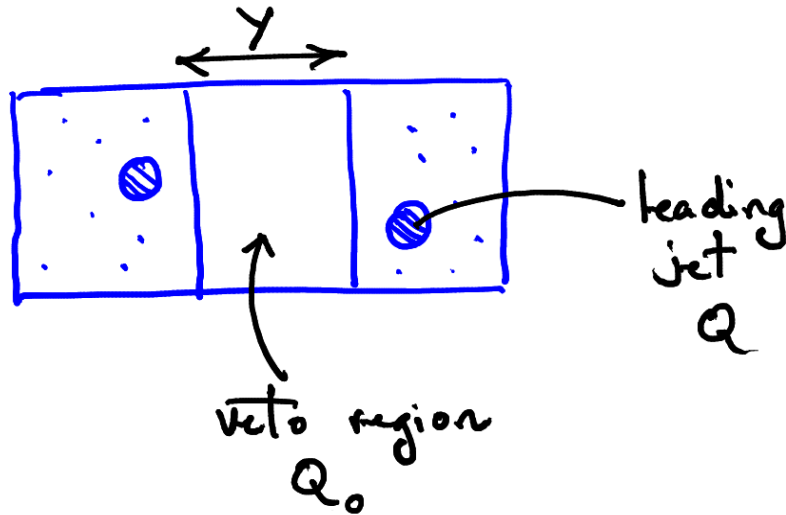
Production near threshold (top, W/Z) ($V = 1 - M^2/\hat{s}$)

Drell-Yan at low p_T (W/Z or Higgs) ($V = p_T^2/\hat{s}$)

Deep-inelastic scattering at large x ($V = 1 - x$)

Gaps between jets....

JET VETOING: “Gaps between jets”



Jets produced with $p_T = Q \gg Q_0$

Observable restricts emission only in the gap region therefore expect

$$\alpha_s^n \log^n(Q/Q_0)$$

i.e. do not expect collinear enhancement since we sum inclusively over the collinear regions of the incoming and outgoing partons.

Real emissions are forbidden in the phase-space region

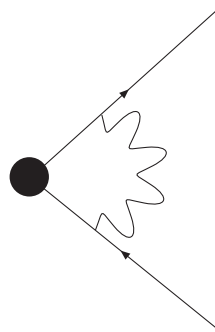
$$-Y/2 < y < Y/2$$

$$k_T > Q_0$$

“By Bloch-Nordsieck, all other real emissions cancel and we therefore only need to compute the virtual soft gluon corrections to the primary hard scattering.”

$e^+e^- \rightarrow q\bar{q}$ case is very simple:

$$\sigma_{\text{gap}} = \sigma_0 \exp\left(-C_F \frac{\alpha_s}{\pi} Y \ln\left(\frac{Q}{Q_0}\right)\right)$$



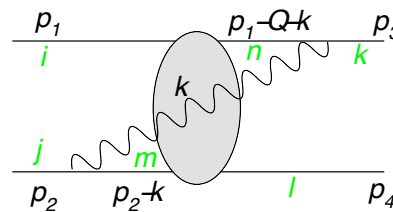
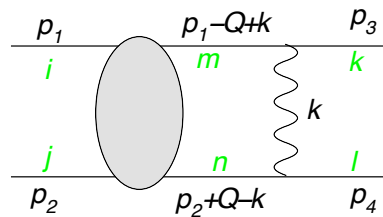
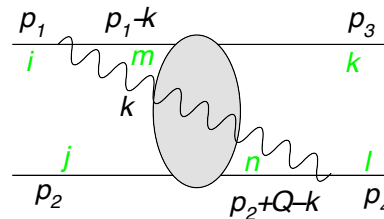
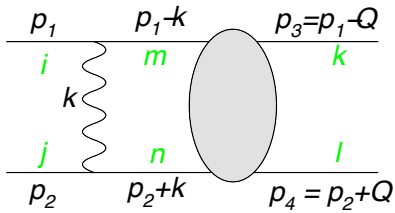
The virtual gluon is integrated over “in gap” momenta, i.e. the region where real emissions are forbidden.

Real emissions are forbidden in the phase-space region

$$-Y/2 < y < Y/2$$

$$k_T > Q_0$$

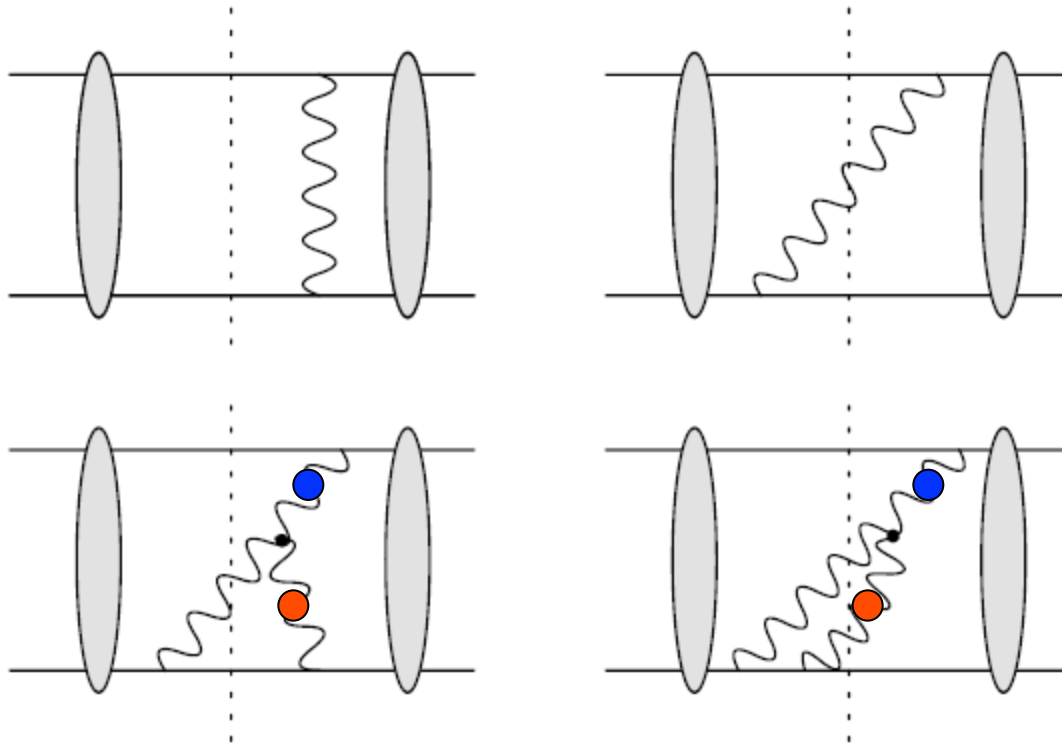
“By Bloch-Nordsieck, all other real emissions cancel and we therefore only need to compute the virtual soft gluon corrections to the primary hard scattering.”



The virtual gluon is integrated over “in gap” momenta, i.e. the region where real emissions are forbidden.

But this is over an oversimplification: we cannot get rid of the real emissions so easily....

This observable is *non-global*



Real & virtual
corrections cancel
for
“out of gap” gluons.

But these do not if
the gluon marked
with a **red** blob is in
the forbidden region:
the 2nd cut is not
allowed.

The observable is sensitive to “out of gap” gluons.

The real emissions no longer cancel once we start to evolve emissions (such as those denoted by the **blue** blob in the above) which lie *outside of the gap* region and which have $k_T > Q_0$.

If $k_T < Q_0$ then subsequent evolution also has $k_T < Q_0$ and cancellation works.

- The observable is sensitive to gluon emissions outside of the gap, even though it sums inclusively over that region.
- Not a surprise: emissions outside of the gap can radiate back into the gap.
- Must include *any number of emissions* outside of the gap and their subsequent evolution.
- Colour structure now becomes much more complicated.

The amplitude can be projected onto a colour basis, e.g. for quark scattering:

$$(M)_{ij}^{kl} = M^{(1)} C_{ijkl}^{(1)} + M^{(8)} C_{ijkl}^{(8)} \quad \begin{aligned} C_{ijkl}^{(8)} &= (T^a)_{ik} (T^a)_{jl} \\ C_{ijkl}^{(1)} &= \delta_{ik} \delta_{jl} \end{aligned}$$

i.e. $\mathbf{M} = \begin{pmatrix} M^{(1)} \\ M^{(8)} \end{pmatrix}$ and $\sigma = \mathbf{M}^\dagger \mathbf{S}_V \mathbf{M}$

$$\mathbf{S}_V = \begin{pmatrix} N^2 & 0 \\ 0 & \frac{N^2-1}{4} \end{pmatrix}$$

Iterating the insertion of soft virtual gluons builds up the resummed amplitude:

$$\mathbf{M} = \exp \left(-\frac{2\alpha_s}{\pi} \int_{Q_0}^Q \frac{dk_T}{k_T} \mathbf{\Gamma} \right) \mathbf{M}_0$$

where the evolution matrix is

$$\mathbf{\Gamma} = \begin{pmatrix} \frac{N^2-1}{4N} \rho(Y, \Delta y) & \frac{N^2-1}{4N^2} i\pi \\ i\pi & -\frac{1}{N} i\pi + \frac{N}{2} Y + \frac{N^2-1}{4N} \rho(Y, \Delta y) \end{pmatrix}$$

Δy = distance between jet centres

Y = size of gap

Further real emissions introduce new ingredients

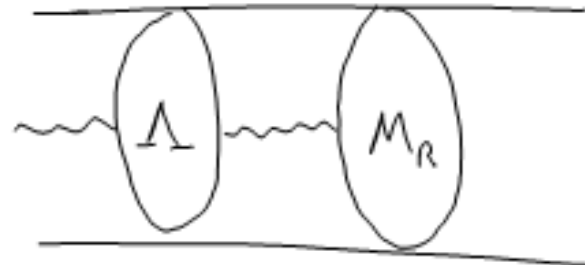
1) How to add a real gluon to the four-quark amplitude

$$\mathbf{M}_R = \mathbf{D} \cdot \mathbf{M}$$



2) How to evolve the resulting 5-parton amplitude

$$\mathbf{M}_R(Q_0) = \exp \left(-\frac{2\alpha_s}{\pi} \int_{Q_0}^{k_T} \frac{dk'_T}{k'_T} \mathbf{\Lambda} \right) \mathbf{M}_R(k_T)$$



$$\mathbf{D}^\mu = \begin{pmatrix} \frac{1}{2}(-h_1^\mu - h_2^\mu + h_3^\mu + h_4^\mu) & \frac{1}{4N}(-h_1^\mu - h_2^\mu + h_3^\mu + h_4^\mu) \\ 0 & \frac{1}{2}(-h_1^\mu - h_2^\mu + h_3^\mu + h_4^\mu) \\ \frac{1}{2}(-h_1^\mu + h_2^\mu + h_3^\mu - h_4^\mu) & \frac{1}{4N}(h_1^\mu - h_2^\mu - h_3^\mu + h_4^\mu) \\ 0 & \frac{1}{2}(-h_1^\mu + h_2^\mu - h_3^\mu + h_4^\mu) \end{pmatrix} \quad h_i^\mu = \frac{1}{2}k_T \frac{p_i^\mu}{p_i \cdot k}$$

$$\mathbf{\Lambda} = \begin{pmatrix} \frac{N}{4}(Y - i\pi) + \frac{1}{2N}i\pi & \left(\frac{1}{4} - \frac{1}{N^2}\right)i\pi & -\frac{N}{4}s_y Y & 0 \\ i\pi & \frac{N}{4}(2Y - i\pi) - \frac{3}{2N}i\pi & 0 & 0 \\ -\frac{N}{4}s_y Y & 0 & \frac{N}{4}(Y - i\pi) - \frac{1}{2N}i\pi & -\frac{1}{4}i\pi \\ 0 & 0 & -i\pi & \frac{N}{4}(2Y - i\pi) - \frac{1}{2N}i\pi \end{pmatrix}$$

$$+ \begin{pmatrix} N & 0 & 0 & 0 \\ 0 & N & 0 & 0 \\ 0 & 0 & N & 0 \\ 0 & 0 & 0 & N \end{pmatrix} \frac{1}{4}\rho(Y, 2|y|)$$

$$+ \begin{pmatrix} C_F & 0 & 0 & 0 \\ 0 & C_F & 0 & 0 \\ 0 & 0 & C_F & 0 \\ 0 & 0 & 0 & C_F \end{pmatrix} \frac{1}{2}\rho(Y, \Delta y)$$

$$+ \begin{pmatrix} \frac{N}{4}\left(-\frac{1}{2}\lambda\right) & 0 & \frac{N}{4}\left(-\frac{1}{2}s_y\lambda\right) & \frac{1}{4}\left(\frac{1}{2}s_y\lambda\right) \\ 0 & \frac{N}{4}\left(-\frac{1}{2}\lambda\right) & 0 & \frac{N}{4}\left(\frac{1}{2}s_y\lambda\right) \\ \frac{N}{4}\left(-\frac{1}{2}s_y\lambda\right) & 0 & \frac{N}{4}\left(-\frac{1}{2}\lambda\right) & \frac{1}{4}\left(-\frac{1}{2}\lambda\right) \\ \frac{1}{2}s_y\lambda & \left(\frac{N}{4} - \frac{1}{N}\right)\left(\frac{1}{2}s_y\lambda\right) & -\frac{1}{2}\lambda & \frac{N}{4}\left(-\frac{1}{2}\lambda\right) \end{pmatrix}$$

The general algorithm

$$\sigma = \sum_{n=0}^{\infty} \int d\sigma_n F_n$$

$$d\sigma_0 = \langle M^{(0)} | \mathbf{V}_{0,Q}^\dagger \mathbf{V}_{0,Q} | M^{(0)} \rangle d\Pi_0$$

$$d\sigma_1 = \langle M^{(0)} | \mathbf{V}_{q_{1T},Q}^\dagger \mathbf{D}_{1\mu}^\dagger \mathbf{V}_{0,q_{1T}}^\dagger \mathbf{V}_{0,q_{1T}} \mathbf{D}_1^\mu \mathbf{V}_{q_{1T},Q} | M^{(0)} \rangle d\Pi_0 d\Pi_1$$

$$d\sigma_2 = \langle M^{(0)} | \mathbf{V}_{q_{1T},Q}^\dagger \mathbf{D}_{1\mu}^\dagger \mathbf{V}_{q_{2T},q_{1T}}^\dagger \mathbf{D}_{2\nu}^\dagger \mathbf{V}_{0,q_{2T}}^\dagger \mathbf{V}_{0,q_{2T}} \mathbf{D}_2^\nu \mathbf{V}_{q_{2T},q_{1T}} \mathbf{D}_1^\mu \mathbf{V}_{q_{1T},Q} | M^{(0)} \rangle d\Pi_0 d\Pi_1 d\Pi_2$$

$$\mathbf{V}_{a,b} = \exp \left[-\frac{2\alpha_s}{\pi} \int_a^b \frac{dk_T}{k_T} \sum_{i<j} (-\mathbf{T}_i \cdot \mathbf{T}_j) \frac{1}{2} \left\{ \int \frac{dy d\phi}{2\pi} \omega_{ij} - i\pi \Theta(ij = II \text{ or } FF) \right\} \right]$$

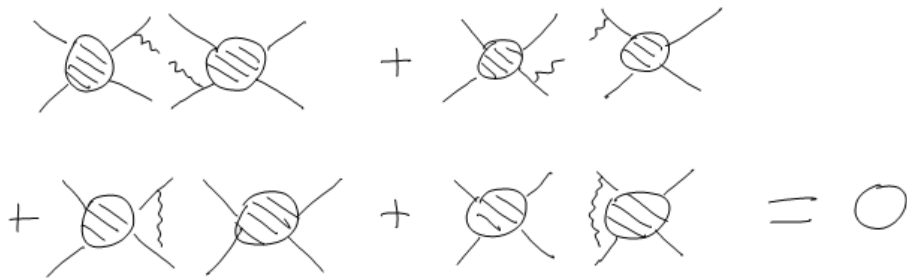
$$\mathbf{D}_i^\mu = \sum_j \mathbf{T}_j \frac{1}{2} q_{Ti} \frac{p_j^\mu}{p_j \cdot q_i},$$

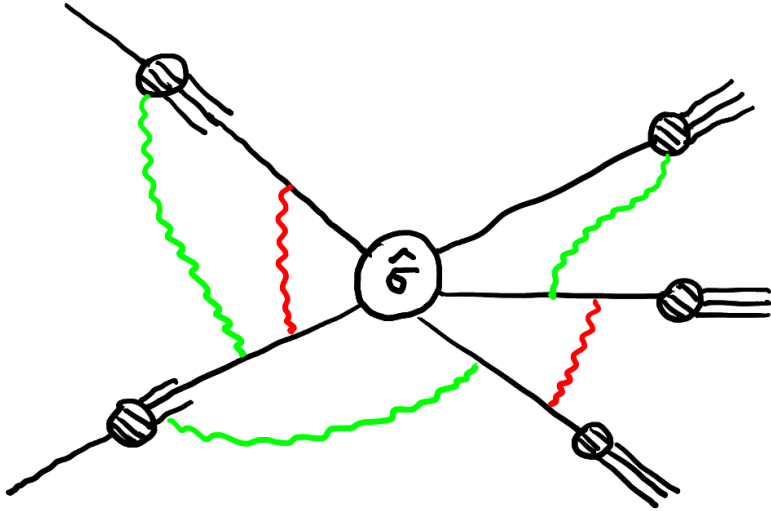
$$d\Pi_i = -\frac{2\alpha_s}{\pi} \frac{dq_{Ti}}{q_{Ti}} \frac{dy_i d\phi_i}{2\pi}.$$

$$\omega_{ij} = \frac{1}{2} k_T^2 \frac{p_i \cdot p_j}{(p_i \cdot k)(p_j \cdot k)}$$

Coulomb gluons a.k.a. Glauber gluons

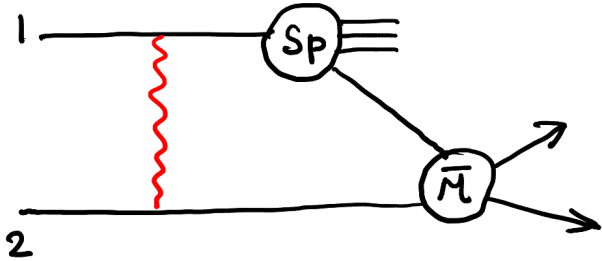
- The real-virtual cancellation of soft gluons occurs point-by-point in phase-space only between the **real parts** of the virtual corrections and the real emissions.
- Below Q_0 , the **imaginary parts** exponentiate to produce a pure phase in the amplitude and no physical effect.
- Above Q_0 , the **imaginary parts** mix with the real parts in non-abelian QCD and contribute.





Coherence allows us to "unhook"
eikonal gluons & recover
collinear factorization.
But it fails for Coulomb gluons.

One loop



$$|\mathcal{M}^{(1)}\rangle = Sp |\bar{\mathcal{M}}\rangle$$

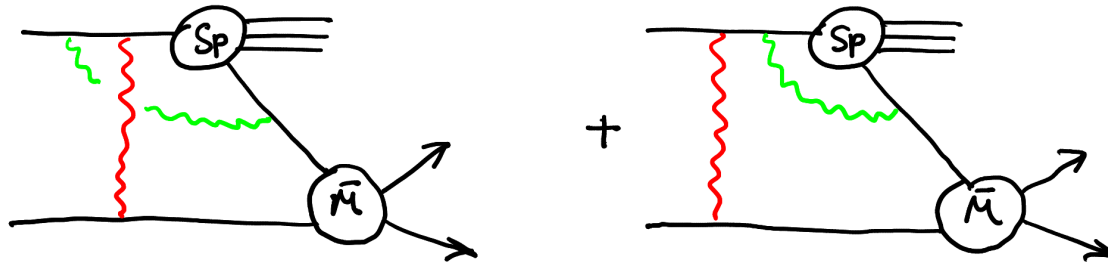
$$Sp \sim i\pi \underline{T}_1 \cdot \underline{T}_2 = \Delta_c$$

$$\text{But } \sigma \sim \langle \mathcal{M}^{(1)} | \mathcal{M}^{(0)} \rangle + \langle \mathcal{M}^{(0)} | \mathcal{M}^{(1)} \rangle$$

So no breakdown of collinear factorization

$\therefore \Delta_c$ is anti-hermitian

Two loops

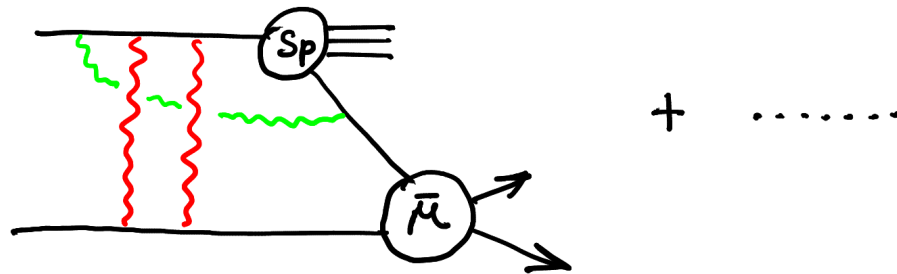


$$Sp \sim [I, \Delta_c]$$

$$\text{But } \sigma \sim \text{Tr} (H [I, \Delta_c]) = 0 \text{ in QCD}$$

\therefore \uparrow symmetric \uparrow anti-symmetric

Three loops

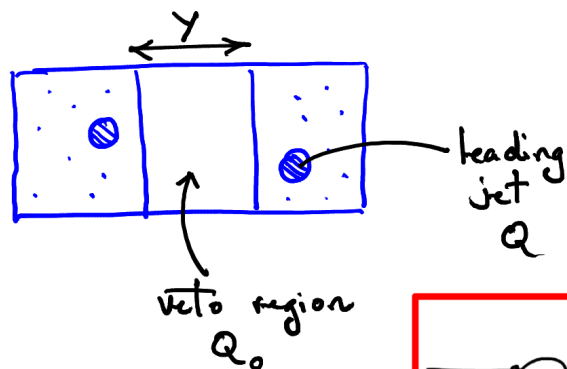


$$Sp \sim [\Delta_c, [\Delta_c, I]]$$

No escape !

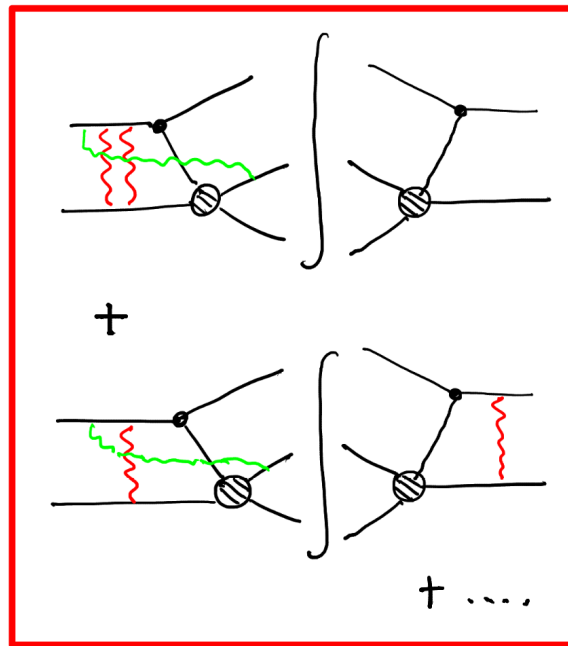
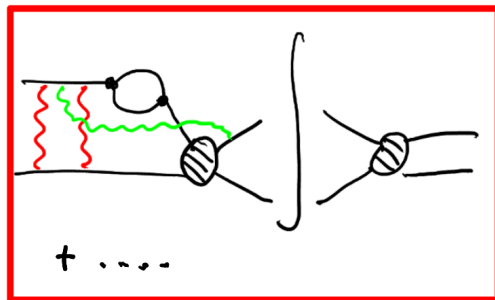
Only cancels if we integrate over the full green (“eikonal”) gluon phase-space, i.e. no breakdown of the factorization theorems as originally proven.

The impact on “gaps between jets”



$$\sigma = \sigma_0 + \sigma_1 + \sigma_2 + \dots$$

$$\sigma_1 = \sigma_1^V - \sigma_1^R$$



$$\sigma_1 \sim \frac{\alpha_s}{\pi} \int_{Q_0}^Q \frac{dk_{\perp}}{k_{\perp}} \int dy \times \pi^2 Y \left[\frac{\alpha_s}{\pi} \int_{Q_0}^{k_T} \frac{dk'_{\perp}}{k'_{\perp}} \right]^3 \times \left\{ t_1^2 \left[\left[t_2^2, \Delta_c \right], \Delta_c \right] - t_1 \left[\left[t_2^2, \Delta_c \right], \Delta_c \right] t_1 \right\}$$

$$\sigma_1 \sim \alpha_s^4 \log^5 \left(\frac{Q}{Q_0} \right) \pi^2 Y$$

Jet vetoing as a tool

Measurement of **electroweak** production of $Z + \text{two jets}$

The signal:

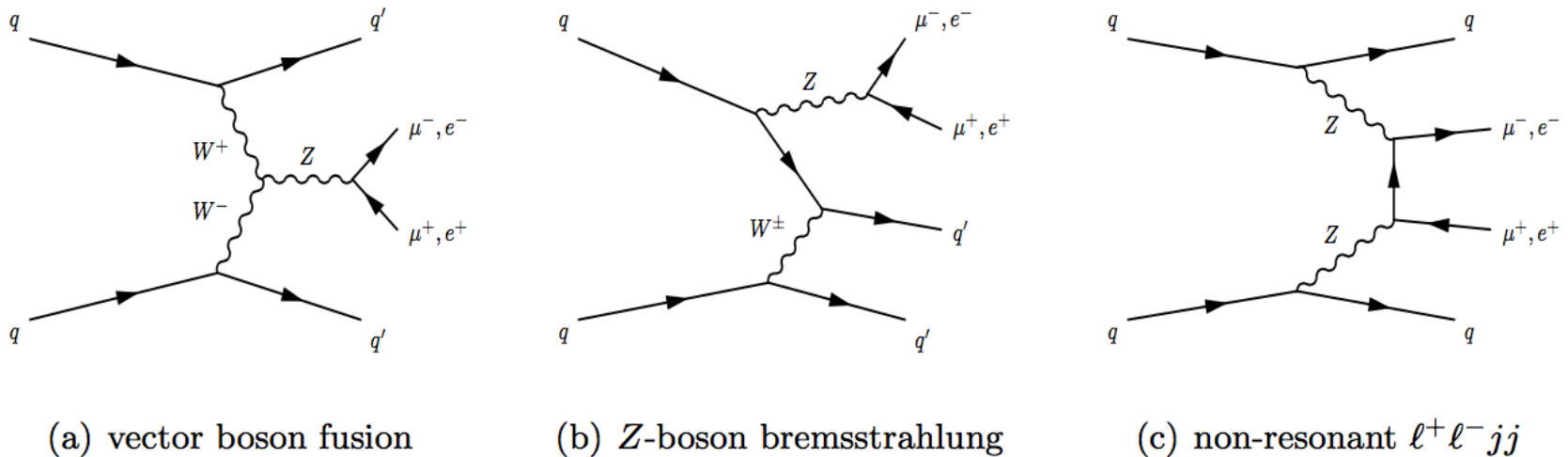
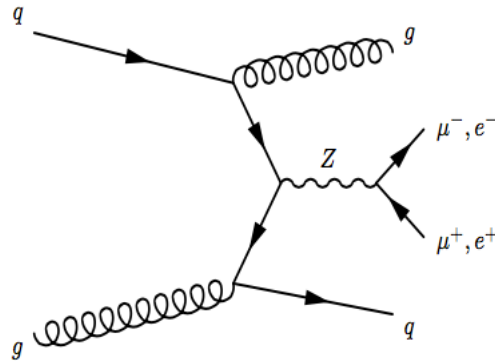


Figure 1. Representative leading-order Feynman diagrams for electroweak Zjj production at the LHC: (a) vector boson fusion (b) Z -boson bremsstrahlung and (c) non-resonant $\ell^+\ell^-jj$ production.

The background:



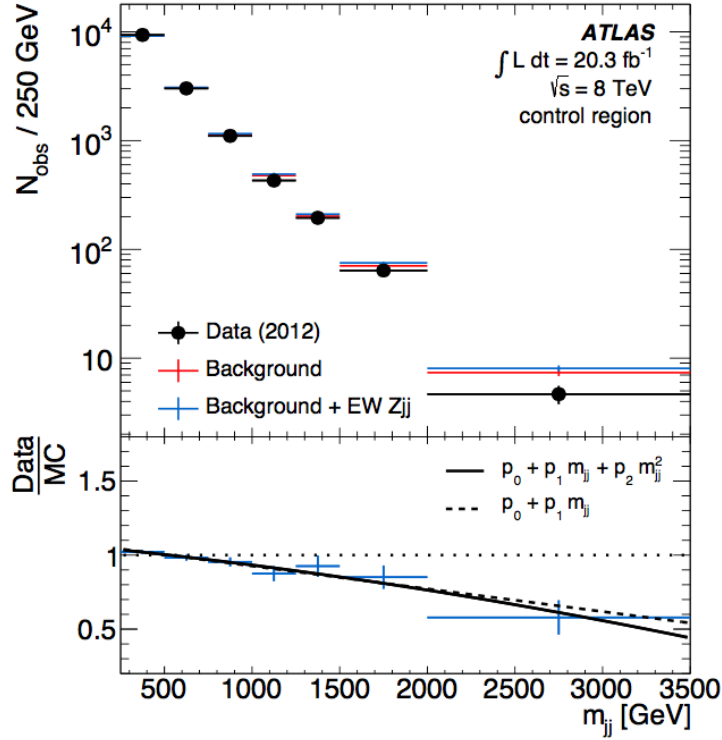
(a) strong Zjj production

The QCD process is much more likely to radiate extra gluons.....so

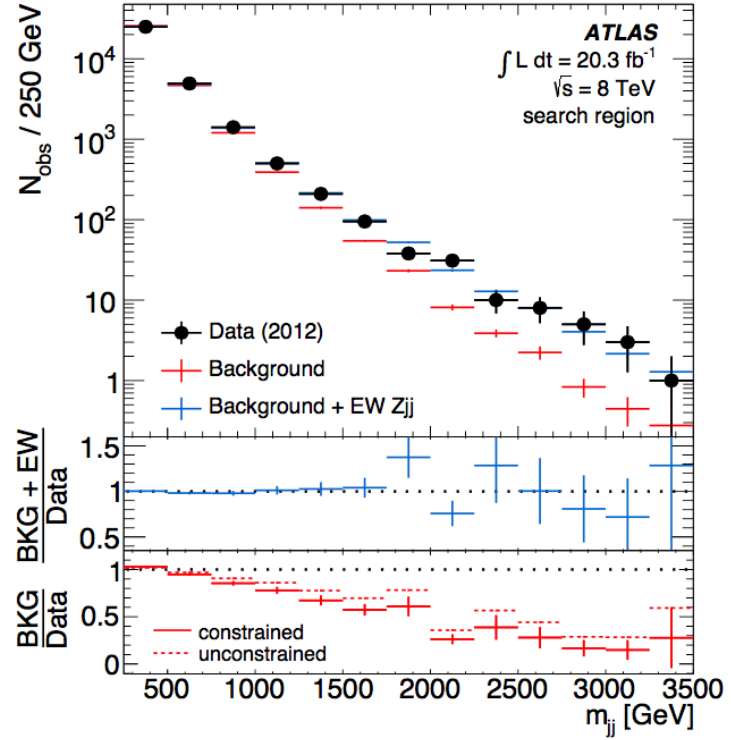
Divide the event sample into two, according to whether or not there is a 3rd jet in between the two highest transverse momentum jets

Signal sample = no 3rd jet

Control sample = a 3rd jet



(a)



(b)

Figure 11. (a) The dijet invariant mass distribution in the *control* region. The simulation has been normalised to match the number of events observed in the data. The lower panel shows the reweighting function used to constrain the shape of the background template. (b) The dijet invariant mass distribution in the *search* region. The signal and (constrained) background templates are scaled to match the number of events obtained in the fit. The lowest panel shows the ratio of constrained and unconstrained background templates to the data.

Since the background is extracted from the data, many of the experimental and theoretical uncertainties associated with it are reduced, e.g.

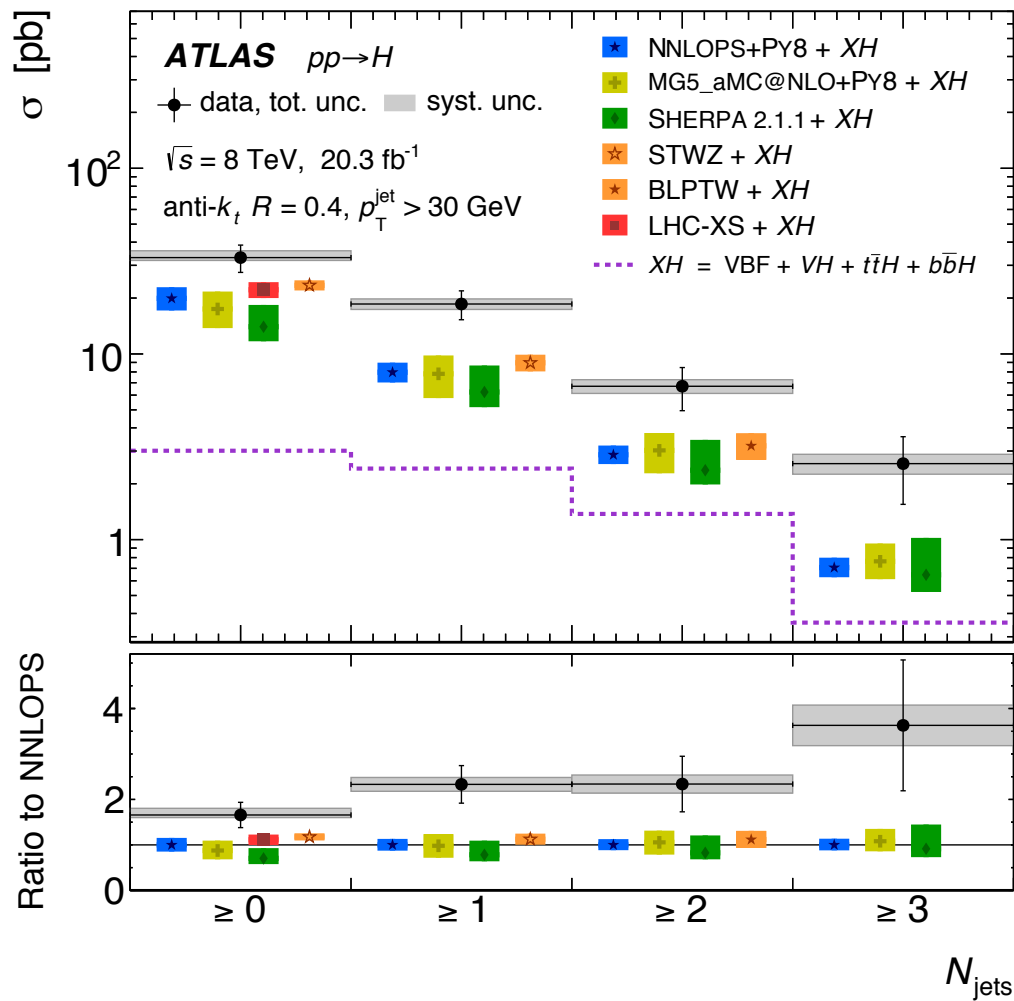
- Theoretical modelling of background is 7.5% (i.e. from using different Monte Carlo generators to provide the template). The theory itself is known far less accurately than this.
- Uncertainty on the energy scale calibration of the jets is down to 5.6% (since it only really affects the shape of the signal). This would otherwise be > 20%.

$$\sigma_{EW} = 54.7 \pm 4.6 \text{ (stat)}_{-10.4}^{+9.8} \text{ (syst)} \pm 1.5 \text{ (lumi) fb}$$

Theory predicts $\approx 46 \pm 1$ fb

Impressively high significance of observation because of the use of the jet veto.

A precursor to similar studies in Higgs production.



Just starting
to study jets in
Higgs production.

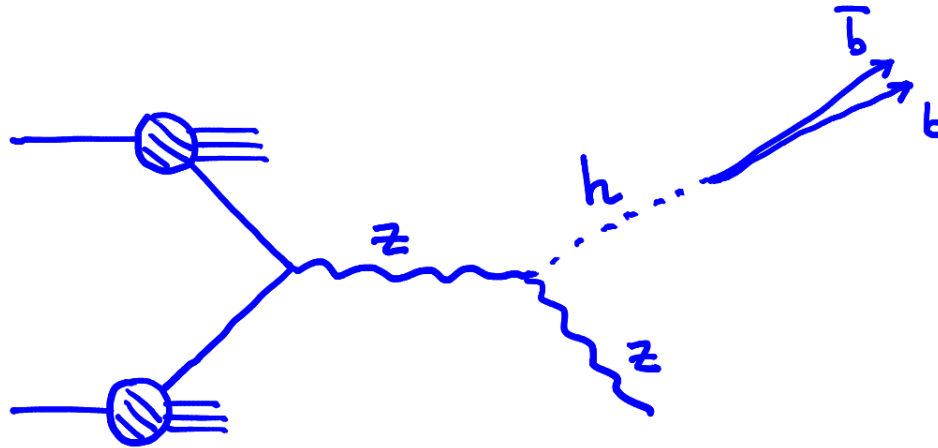
One of the exciting
areas for Run 2.

Absolute and fractional cross sections in bins of jet multiplicity for inclusive Higgs boson production at 8 TeV measured by combining the $H \rightarrow \gamma\gamma$ and $H \rightarrow ZZ^* \rightarrow 4\ell$ analyses using 20.3 fb^{-1} of pp collisions.

ATLAS collaboration arXiv: 1504.05833v2

Jet substructure: a way to detect boosted heavy particles

e.g.

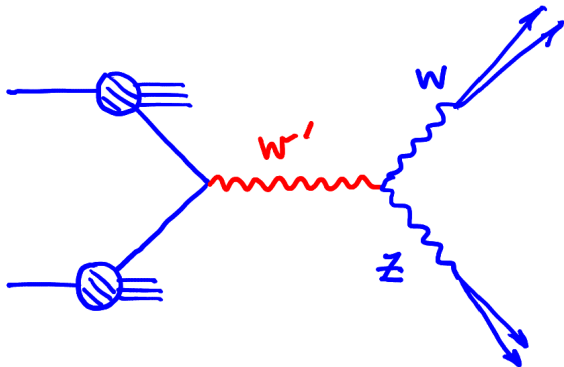
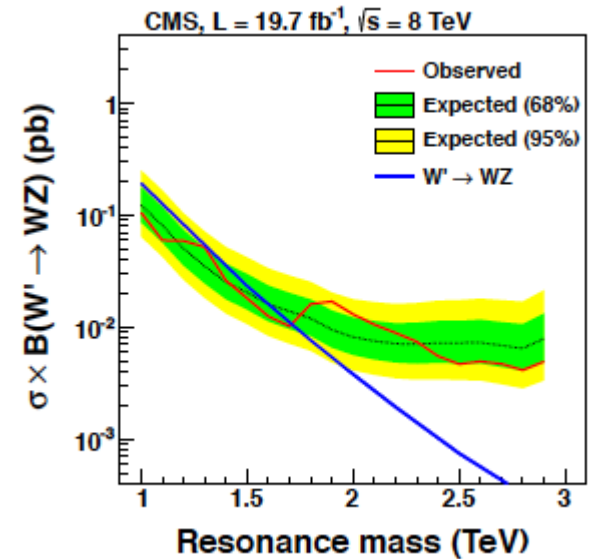
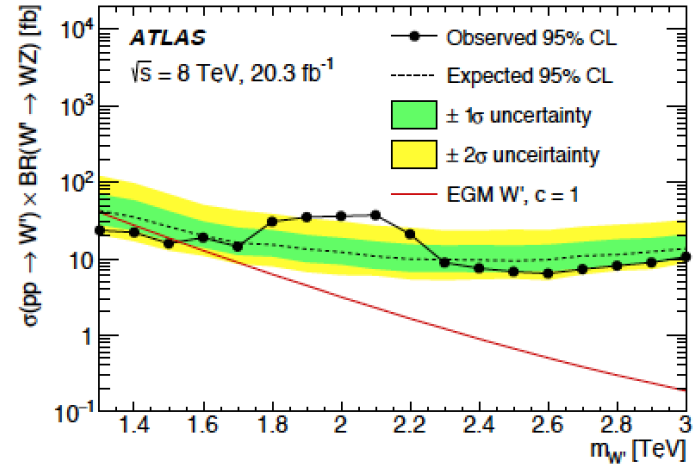
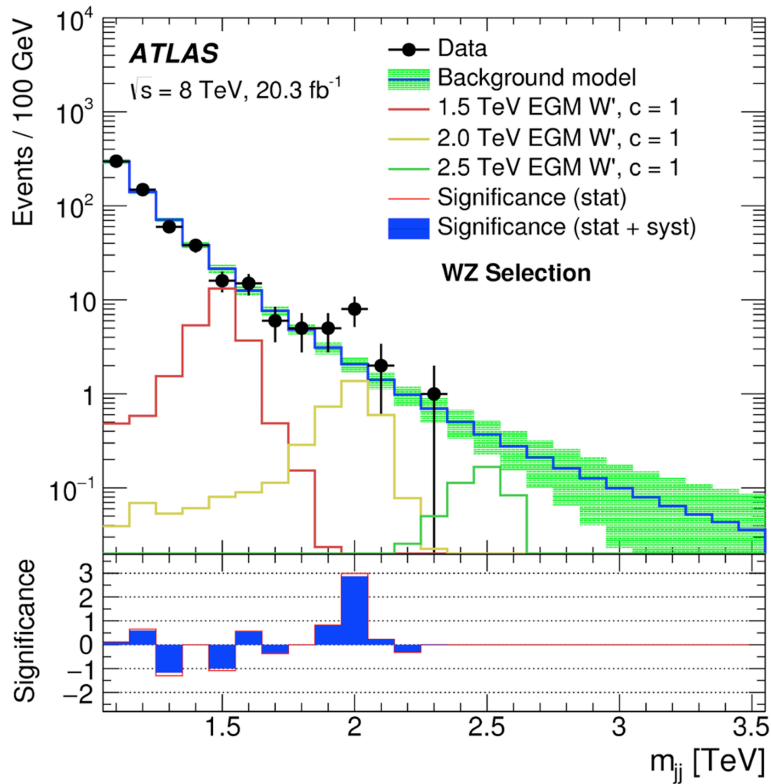


Not used to date (8 TeV) in Higgs decay to b quarks but expected to be important in 14 TeV analyses and the eventual detection. Butterworth, Ochoa, Scanlon [arXiv: 1506.04973](https://arxiv.org/abs/1506.04973)

Butterworth, Davison, Rubin, Salam [arXiv:0802.2470](https://arxiv.org/abs/0802.2470)
Seymour, Z. Phys. C 62, 127 (1994)
Butterworth, Cox and JRF, hep-ph/0201098

Major progress on analytic understanding of jet substructure:
Dasgupta, Fregoso, Marzani, Salam [arXiv:1307.0007](https://arxiv.org/abs/1307.0007)
Dasgupta, Fregoso, Marzani, Powling [arXiv:1307.0013](https://arxiv.org/abs/1307.0013)

A 3.4σ bump!?



Conclusions

- Accounting for soft gluons is hampered by the complications of colour.
- Partial resummations, based on parton shower Monte Carlo, are subject to potentially large corrections, especially from sub-leading colour and Coulomb gluons.
- Features of QCD radiation can be used to isolate and study non-QCD physics. This will be a feature of LHC Run 2 analyses.